Article

pubs.acs.org/Biomac

Sericin Promotes Fibroin Silk I Stabilization Across a Phase-Separation

Hyo Won Kwak,[†,‡] Ji Eun Ju,[†] Munju Shin,[†] Chris Holland,[§] and Ki Hoon Lee*[,†,∥,⊥]

[†]Department of Biosystems and Biomaterials Science and Engineering, Seoul National University, Seoul 151-921, Korea
[§]Department of Materials Science and Engineering, The University of Sheffield, Sheffield, S1 3JD, United Kingdom
[∥]Research Institute of Agriculture and Life Sciences, Seoul National University, Seoul 151-921, Korea
[⊥]Center for Food & Bioconvergence, Seoul National University, Seoul 151-921, Korea

Supporting Information

ABSTRACT: Natural silk spinning offers several advantages over the synthetic fiber spinning, although the underlying mechanisms of this process are yet to be fully elucidated. Silkworm silks, specifically *B. mori*, comprise two main proteins: fibroin, which forms the fiber, and sericin, a coextruded coating that acts as a matrix in the resulting nonwoven composite cocoon. To date, most studies have focused on fibroin's self-assembly and gelation, with the influence of sericin during spinning receiving little to no attention. This study investigates sericin's effects on the self-assembly of fibroin via their natural phase-separation. Through changes in sample opacity, FTIR, and XRD, we report that increasing sericin concentration retards the time to gelation and β-sheet formation of fibroin, causing it to adopt a Silk I conformation. Such findings have important implications for both the natural silk spinning process and any future industrial applications, suggesting that sericin may be able to induce long-range conformational and stability control in silk fibroin, while being in a separate phase, a factor that would facilitate long-term storage or silk feedstocks.

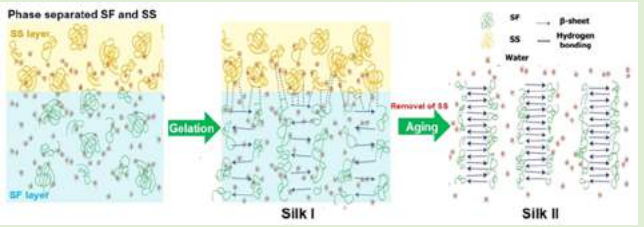

1. INTRODUCTION

The mulberry silkworm, *Bombyx mori* silk, has been widely used in industry due to its broad domestication, overall quality, and more recently, for use in high tech applications.[1−3] However, despite its utility, certain details of the natural spinning process represent a gap in our knowledge. When comparing the natural spinning process to industrial approaches, silk spinning appears to be a type of dry spinning, wherein a protein solution is moved through a silk gland, solidifies into a fiber and is then excreted.[4,5] This secreted fiber is used by the silkworm *B. mori* to form a protective cocoon prior to metamorphosis and is a continuous strand composed of two proteins, namely, fibroin and sericin. Fibroin constitutes 75% of the fiber strand weight and functions as the structural component, the remaining 25%, sericin, a group of polypeptides, has been assigned a minor role and is thought to be simply a protein that glues fibroin threads together during cocoon construction.[6,7]

During the silk spinning process, silk dope solution undergoes changes in its composition and physical state.[8,9] For this reason, much attention has been focused on the physiological condition such as pH, ion concentration, temperature, and external forces on the self-assembly of fibroin.[10,11] However, recently, there is evidence to suggest there may be a further role for silk sericin in this process. Ki et al.[12] reported the effect of sericin on the secondary structure of fibroin during wet spinning, and Hang et al.[13] suggested some interaction between sericin and fibroin during coaxial electrospinning. However, the most compelling evidence to date comes from Lee[14] who observed micelle structures in a blended film of fibroin and sericin and speculated that the hydrogen bonds between fibroin and sericin retard the β-sheet crystallization of fibroin. However, while dry films are clearly different to the natural liquid state of the proteins found in the silk gland, this work does suggest that sericin may influence and perhaps even mediate the solidification kinetics and structure of fibroin.

Therefore, the focus of this study is to mimic and understand the interaction between sericin and fibroin during storage, as opposed to the spinning. To this end, we have investigated the interaction between fibroin and sericin in solution. Using these protein's natural propensity for macrophase-separation, we have been able to control the concentration of sericin and determine the impact it has on gelation and β-sheet conformational transition kinetics of fibroin.

2. MATERIALS AND METHODS

2.1. Materials. *Bombyx mori* silkworm cocoons were kindly provided by National Academy of Agricultural Science. Formic acid, sodium carbonate (Na_2CO_3), sodium oleate, and calcium chloride

Received: April 18, 2017
Revised: June 7, 2017
Published: June 12, 2017

DOI: 10.1021/acs.biomac.7b00549
Biomacromolecules 2017, 18, 2343−2349

($CaCl_2$) were purchased from Sigma-Aldrich (U.S.A.). Lithium bromide (LiBr) was purchased from Acros (U.S.A.). Other reagents were purchased from Sigma-Aldrich (U.S.A.).

2.2. Methods. *2.2.1. Preparation of Regenerated Aqueous Fibroin and Sericin Solution.* Silk cocoons were degummed twice with 0.02% (w/v) sodium carbonate and 0.03% (w/v) Marseille soap solution at 100 °C for 30 min, then rinsed with distilled water to remove residual sericin. Following this, the fibroin was dried in an oven at 50 °C.

To obtain high molecular weight, undegraded sericin, the urea/mercaptoethanol extraction method was used on cocoons that had been cut into small pieces.[15] In brief, the cocoon pieces were immersed in a 5% (v/v) 2-mercaptoethanol in 8 M urea solution and heated to 80 °C for 10 min, then the sericin containing solution was filtered through a nonwoven filter to remove any remaining pieces of cocoon. The solution was then dialyzed in distilled water using a cellulose membrane (molecular weight cut off = 6000−8000 Da, Spectrum Laboratories, Inc.) for 2 days to remove residual urea and mercaptoethanol. Finally, the extracted sericin solution was lyophilized and stored in desiccator prior to use.

For the preparation of aqueous regenerated fibroin and sericin solutions, the solid extracted fibroin (10%, w/v) and sericin (2%, w/v) materials were dissolved in a 9.3 M LiBr solution separately at 50 °C for 4 h. The solution was then dialyzed in distilled water with a cellulose membrane for 2 days to remove the residual LiBr. To assess the removal of LiBr after dialysis, conductivity of the dialysate was checked every time until it had the same value as distilled water. The final fibroin and sericin concentration was adjusted 4%, 1% (w/v) with distilled water, respectively.

2.2.2. Gelation Experiment of Fibroin. To monitor the gelation of fibroin with phase-separated sericin, 10 mL of aqueous fibroin solution was added to an empty 20 mL vial. Then, 5 mL of distilled water and aqueous sericin (0, 0.25, 0.50, and 1.00%, w/v) with 100 ppm of rhodamine B dye was carefully added above the fibroin solution using a syringe pump (KD Scientific, U.S.A.) in order to maintain the interface between the two solutions (Figure 1). Following this, the phase-separation fibroin and sericin samples incubated at 50 °C were observed using a digital camera until gelation had occurred in each fibroin solution.

In a separate experiment, gelation kinetics were investigated using a microplate reader (Synergy H1, Biotek, U.S.A.) measuring sample turbidity changes at 550 nm as a result of heterogeneous microstructures causing an increase in the degree of light scattering. Using a 24-well plate, per well, 2.0 mL of aqueous fibroin was added, and then 1.0 mL of distilled water or aqueous sericin with various concentrations (0, 0.25, 0.50, and 1.00%, w/v) was added to the above the fibroin solution. As controls, bovine serum albumin (BSA, 1%, w/v) and polyethylene glycol (PEG 200 K, 1%, w/v), were selected. Gelation time was defined as the time from the beginning of incubation at 50 °C to the point when the plateau of optical density was reached.[16]

A fluorescence spectrum (FLS) was also recorded using the above microplate reader. For fluorescence measurements, 20 μM of thioflavin T (ThT) was added to the fibroin (4%, w/v) solution and black plates used (Vision plate 24, 4titude, United Kingdom). The excitation wavelength was set at 420 nm and the emission readings were taken at 480 nm. Time interval for the gelation kinetics was 1 h. Relative gelation kinetics was obtained by the following:

$$\beta\text{-sheet transition kinetics}(\%) = \frac{\text{intensity}_{SF_t} - \text{intensity}_{SF_s}}{\text{intensity}_{SF_g} - \text{intensity}_{SF_s}} \times 100$$

where intensity_{SF_g} = fluorescence intensity of fibroin when gelation completed; intensity_{SF_s} = fluorescence intensity of fibroin solution at time 0; and intenstity_{SF_t} = fluorescence intensity of fibroin solution at time *t*.

2.2.3. Characterization of Fibroin Solution and Hydrogel. 2.2.3.1. Fourier-Transform Infrared (FTIR) Spectroscopy. Fibroin solutions and hydrogels were lyophilized and turned into pellets

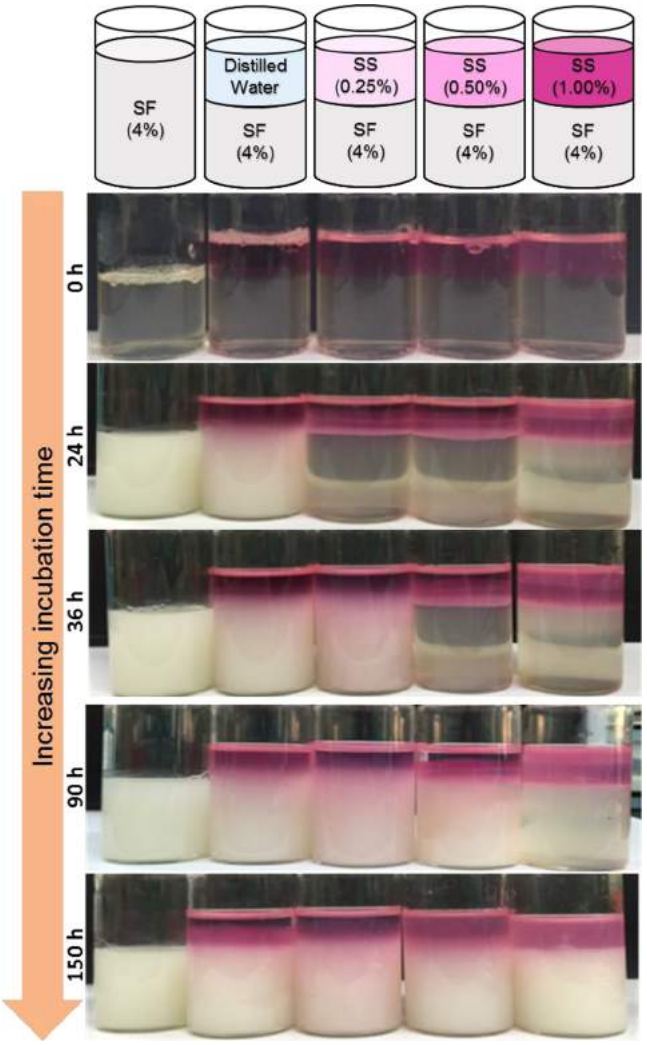

Figure 1. Typical experimental setup to observe the gelation time of silk fibroin (SF) as a result of a phase-separated silk sericin (SS) layer above.

(diameter <13 mm) using a pellet press (The PIKE Technologies, U.S.A.) prior to ATR-FTIR characterization of the amide I band between 1600−1700 cm^{-1} (FTIR Nicolet iS5 with ATR accessory, Thermo Scientific, U.S.A.). For each measurement, 128 scans were taken with a resolution of 4 cm^{-1}. Aquired spectra were first subjected to a baseline correction using a straight line between 1600 and 1700 cm^{-1} and then a nine-point multipeak Gaussian fitting was performed using Origin software with structures assigned according to previous studies[17−19] and the relative area of the single bands underneath the amide I region (Table 1).

2.2.3.2. X-ray Diffraction (XRD). After ATR-FTIR characterization, the same sample pellets were subjected to X-ray diffraction (XRD) using an X-ray diffractometer (D8 DISCOVER, Bruker, U.S.A.) with Cu Kα radiation. Irradiation conditions were 40 kV and 40 mA. XRD

Table 1. FTIR Band Assignments in the Amide I Region for *B. mori* Silk Fibroin[17−19]

wavenumber (cm^{-1})	secondary structure
1605−1615	aggregated strands
1616−1637	β-sheet
1638−1655	random coil
1656−1662	α-helices
1663−1696	β-turns

DOI: 10.1021/acs.biomac.7b00549
Biomacromolecules 2017, 18, 2343−2349

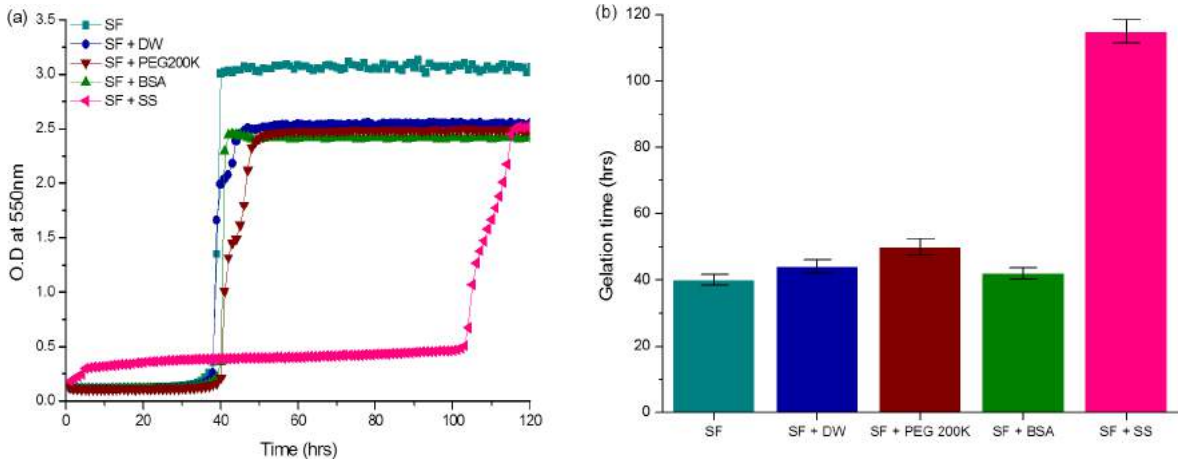

Figure 2. Silk fibroin (SF) gelation delay with various polymers (1%) in the layer above SF (SF at 4%). (a) Representative optical density changes and (b) gelation time of various SF solutions. The error bars represent the s.d. of the different observations (N = 4).

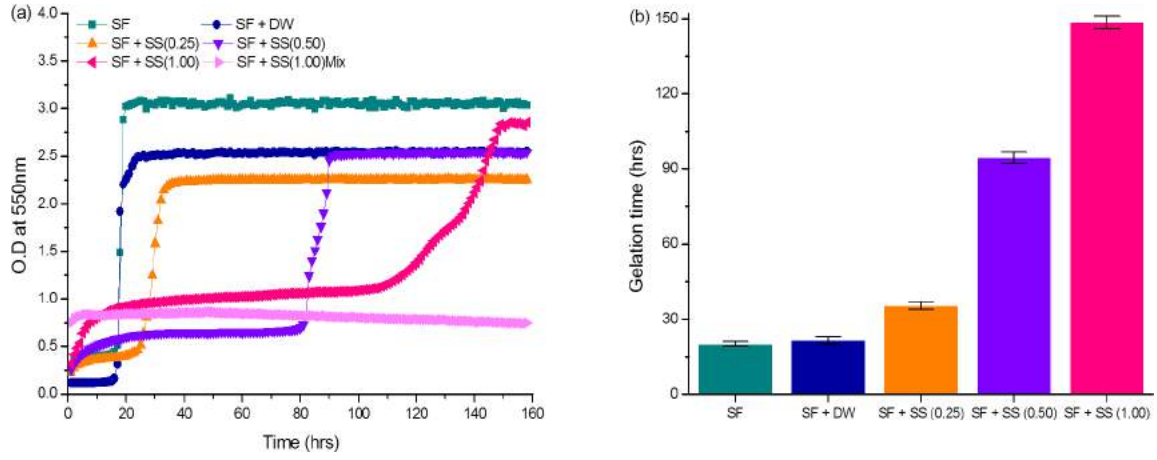

Figure 3. Silk fibroin (SF) gelation delay with various concentrations of silk sericin (SS) on top of SF (4%, w/v): (a) representative optical density changes and (b) gelation time of various SF solutions. The error bars represent the s.d. of the different observations (N = 4).

patterns were recorded at a speed of 2°/min at 40 kV and 35 mA in the region of 2θ from 5° to 40°.

2.2.3.3. Mechanical Tests. To investigate the mechanical properties of fibroin hydrogels, a uniaxial compression experiment was performed. Cylindrical hydrogels with flat and parallel surfaces 15 mm in diameter and 10 mm high were prepared and allowed to swell in distilled water for 24 h prior to testing. The samples were then removed from the water and subjected to compression tests at room temperature using a Universal Testing Machine (Lloyd Instruments, Ltd., United Kingdom) equipped with a 500 N load cell and a cross head speed of 10 mm/min. A total of four hydrogels were tested for each treatment (N = 4).

2.2.3.4. Dissolution and Enzymatic Degradation Test. Lyophilized fibroin hydrogel samples weighing 15 mg (±1 mg) were incubated at 37 °C in phosphate-buffered saline (PBS) solution containing 1 U/mL α-chymotrypsin from human pancreas in 1.5 mL microcentrifuge tubes. As a control, samples were also incubated in PBS at 37 °C without enzymes investigate the dissolution properties of fibroin in PBS. After 1 day of incubation, samples were centrifuged at 10000 rpm for 10 min, and the remaining silk pellet was washed twice with distilled water. After rinsing, fibroin residues were centrifuged again at 10000 rpm for 10 min. The fibroin pellets were dried overnight in a fume hood and the mass determined using a four-point analytical balance. Four samples from each group were taken at each time point (N = 4).

3. RESULTS AND DISCUSSION

To mimic the in vivo interactions between these silk proteins, we used fibroin and sericin's natural tendency to phase-separate. During the silkworm's fifth and final instar, fibroin is secreted into the posterior division silk gland and migrates into the middle division silk gland where sericin begins to be secreted.[20] From this point, both fibroin and sericin are stored as separate phases until spinning, and even after spinning they remain phase-separated.[21] Oh et al.[22] found that the phase-separated state of fibroin and sericin could be maintained in vitro when the sericin solution was carefully loaded onto the top of the fibroin solution without disturbing the interface. While the concentration of silk protein in the silk gland is around 24%,[8] a regenerated sericin solution of more than 1% (w/v) easily converts into a gel state before the phase-separated gelation experiment is begun. For this reason, 1% (w/v) sericin was selected as the limit for this experiment and matched with a 4% (w/v) fibroin solution in order to maintain the natural ratio of sericin to fibroin, as found in the fiber.

In this study, rhodamine B dye, which has a strong affinity for fibroin, was used to monitor the interface between the two proteins during the gelation of fibroin.[23,24] Figure 1 shows the phase-separation state of fibroin (4.0%, w/v) and various concentrations of sericin (0, 0.25, 0.50, 1.0%, w/v) alongside

DOI: 10.1021/acs.biomac.7b00549
Biomacromolecules 2017, 18, 2343−2349

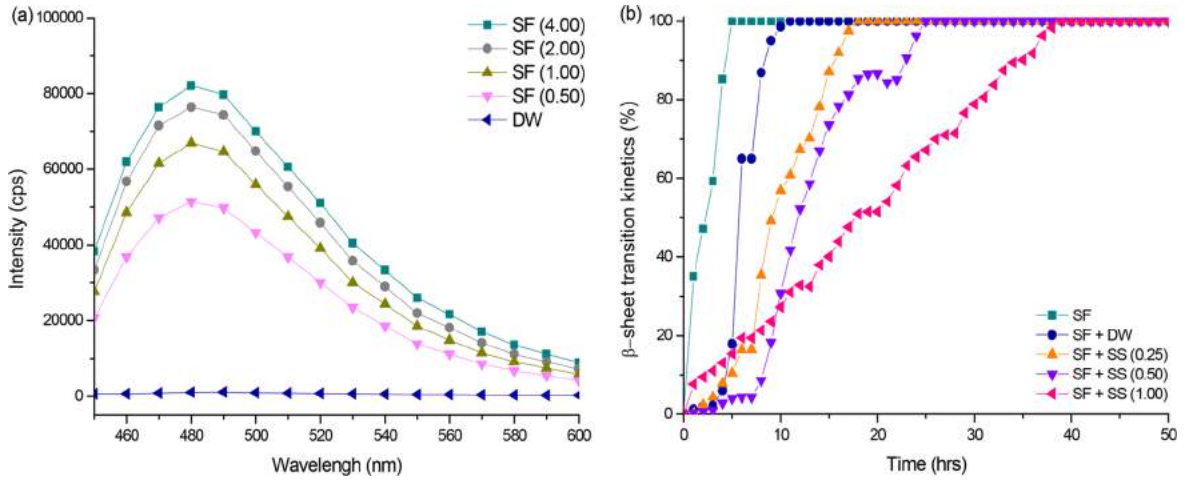

Figure 4. Relative β-sheet transition kinetics of silk fibroin (SF) based on Thioflavin T (ThT) fluorescence intensity. (a) Fluorescence emission spectra of ThT in distilled water and in various concentrations of SF solution. (b) Relative β-sheet transition kinetics of SF (4% w/v) based on ThT fluorescence intensity.

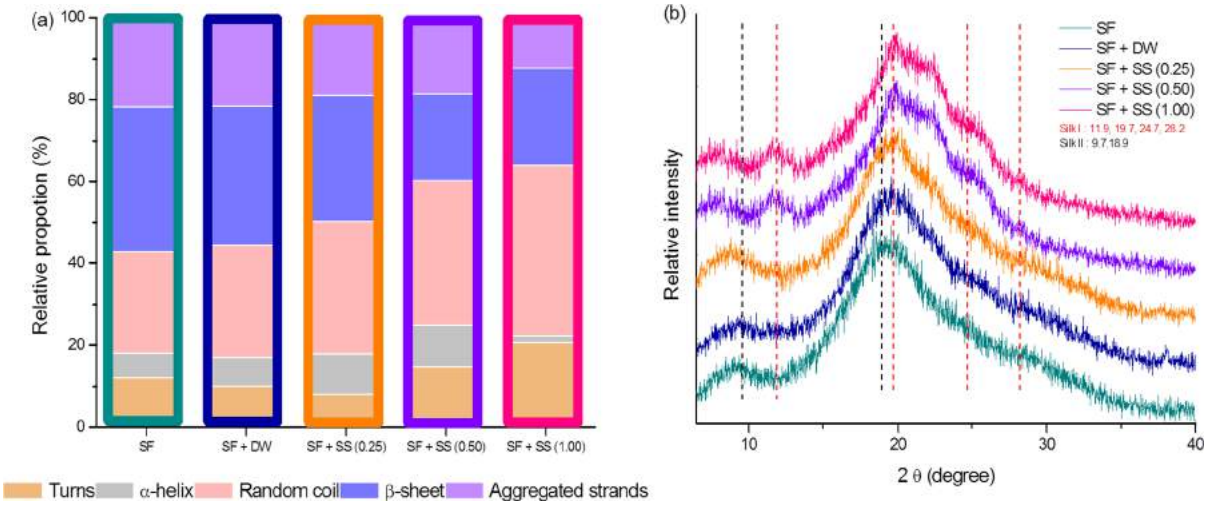

Figure 5. Effect of phase-separated silk sericin (SS) on silk fibroin (SF) gel's secondary structure derived from IR measurements (a) and XRD spectra (b).

the gelation behavior of fibroin over time. During these tests, the rhodamine B dye did not diffuse into the fibroin layer, indicating that the phase-separation between silk proteins was maintained in a liquid state until gelation (as seen by an increase in opacity of the fibroin phase). In addition to the use of an indicator dye, a control to check for protein migration across the layers was performed by testing for variations in dry weight concentration of fibroin and sericin layers before and after the gelation of fibroin (Figure S1). In all cases, variations in concentration before and after were negligible and within the standard deviation of the measurements, suggesting no significant migration of proteins between phases. Comparing across samples, it was clear that the gelation of fibroin was delayed as the concentration of phase-separated sericin increased. This suggests that the sericin phase might play a significant role in the gelation kinetics of fibroin.

This relationship was then investigated in more detail using an optical spectrometer. For comparison, other polymers, such as bovine serum albumin (BSA) and synthetic polyethylene glycol (PEG 200 K), were selected as controls for the experiment (Figure 2). Here the gelation time of the fibroin solution alone and with phases of distilled water, BSA, or PEG 200 K was nearly 40 h. However, the gelation time of fibroin was nearly 3× slower (115 h) when sericin was present in the upper layer, strongly indicating that sericin in particular can retard the gelation behavior of fibroin solutions.

To confirm observations from Figure 2, to determine the effect of the sericin concentration in the upper layer on the gelation of fibroin (4.0%, w/v), various sericin concentrations (0%, 0.25%, 0.50%, 1.00%, w/v) were prepared and tested (Figure 3). Again, the fibroin gelation time increased with increasing sericin concentrations (the effect of different concentrations of fibroin may be found in Figure S2). However, these results cannot completely exclude the possibility that fibroin and sericin mix when the concentration gradient or relative density is not high enough to permit phase-separation. Interestingly, when fibroin and sericin were mixed as a homogeneous solution, gelation did not occur until 160 h. These results imply that sericin can clearly delay the gelation time of fibroin, even though they are phase-separated.

Next we investigated the mechanism of fibroin gelation by using Thioflavin T (ThT), a benzo-thiazole extrinsic

DOI: 10.1021/acs.biomac.7b00549
Biomacromolecules 2017, 18, 2343−2349

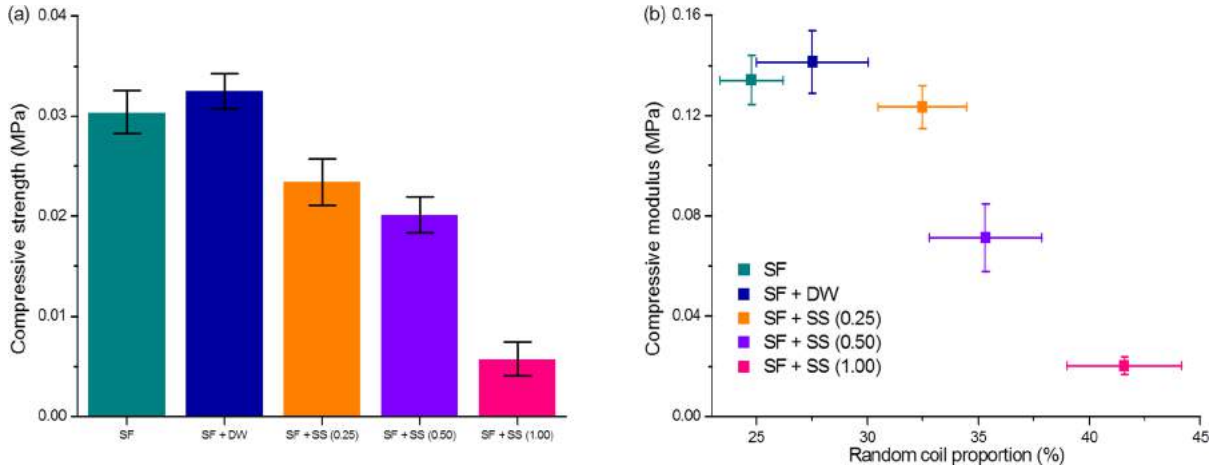

Figure 6. Effect of phase-separated silk sericin (SS) concentration on the mechanical properties of silk fibroin (SF) hydrogel: (a) compressive strength and (b) relationship between random coil structure proportion and compressive modulus. The error bars represent the s.d. of the different observations (N = 4).

fluorescence dye, which enables β-sheet formation to be monitored.[25−28] Free ThT in an aqueous solution shows only weak fluorescence, with lower excitation and emission maxima at 350 and 440 nm, respectively. However, when ThT interacts with β-sheet-rich samples, it generates strong (red-shifted) fluorescence, with excitation and emission maxima at approximately 440 and 490 nm, respectively.[29] Figure 4a shows that, while the initial conformation of the fibroin solutions is mainly random coil, there is some β-sheet content present, and the intensity of fluorescence was increased in proportion to the amount of fibroin. Figure 4b shows the β-sheet transition kinetics of fibroin solution (4%, w/v) in the presence of phase-separated sericin at different concentrations. This clearly indicates that the gelation of fibroin occurred with the conformational transition to β-sheets.[16,30] The results agree well with previous studies, and we can now associate an increase in β-sheet content with gelation of fibroin. In addition, the transition into a β-sheet structure was also retarded if the concentration of the sericin layer increased.

In order to obtain further structural information about fibroin gelation during the phase-separated experiments, fibroin solutions were collected from the bottom layer of the sample container after 1 h, lyophilized, and subjected to ATR-FTIR and XRD analysis. Both tests indicate no significant structural differences at the bottom layer between samples after 1 h and confirmed a mainly random coil/an amorphous state of fibroin (Figure S3).

However, post-gelation, ATR-FTIR and XRD revealed significant differences between samples (Figure 5). FTIR-ATR results show that, as the concentration of the overlying sericin phase increased, random coils and β-turn structures develop at the expense of β-sheets, α-helices, and aggregated strands. XRD results provided more insight into this situation, with data indicating that an increasing sericin concentration promotes a Silk I conformation of fibroin to develop in the gel rather than the typical Silk II.[31,32]

Furthermore, if the sericin layer is removed post-gelation and the fibroin gels allowed to stand for 2 days, all samples converted to a Silk II structure (Figure S4). Thus, it can be concluded that phase-separated sericin retards fibroin Silk II formation by stabilizing Silk I structures but does not induce a permanent change in the gel.

SF Gel Post-Gelation with Phase-Separated Sericin. Further evidence to support sericin's ability to influence the properties of fibroin gels were obtained by investigating fibroin's mechanical properties and degradation profile. Figure 6 shows the compressive strength and modulus of fibroin hydrogels prepared with different upper phase concentrations of sericin. At the same fibroin concentrations, the mechanical properties of the fibroin hydrogel were found to decrease with increasing concentrations of sericin. This also coincides with changes in the secondary structure composition analysis by FTIR and XRD. This is also consistent with other studies on hydrogel mechanical properties which have shown that a greater proportion of random coil structures may be responsible for a weaker hydrogel.[33−35]

Since the random coil-rich, amorphous regions of fibroin are water-soluble and degradable, they are prone to both dissolution and proteolytic enzymes,[36] while the Silk II crystalline region of fibroin is not.[37] Therefore, after gelation and lyophilization, both PBS and α-chymotrypsin were used to investigate fibroin hydrogel degradation. Figure 7 and Figure S5 show that all fibroin hydrogels exhibiting either Silk I or Silk II

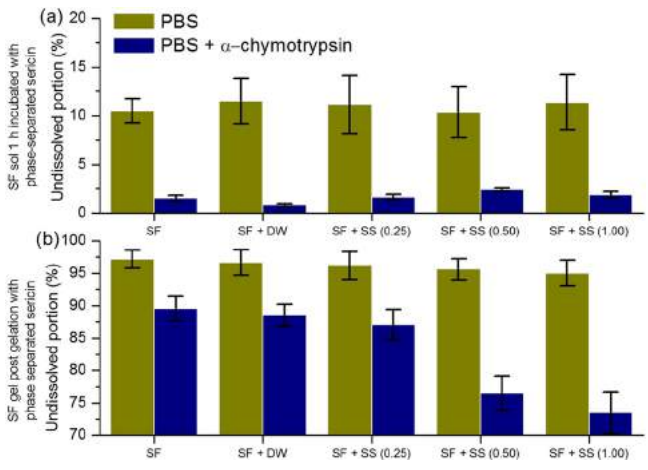

Figure 7. Water dissolution and enzymatic degradation properties of silk fibroin (SF) sol (a), SF gel phase-separated with different concentration of silk sericin (SS) (b). The error bars represent the s.d. of the different observations (N = 4).

DOI: 10.1021/acs.biomac.7b00549
Biomacromolecules 2017, 18, 2343−2349

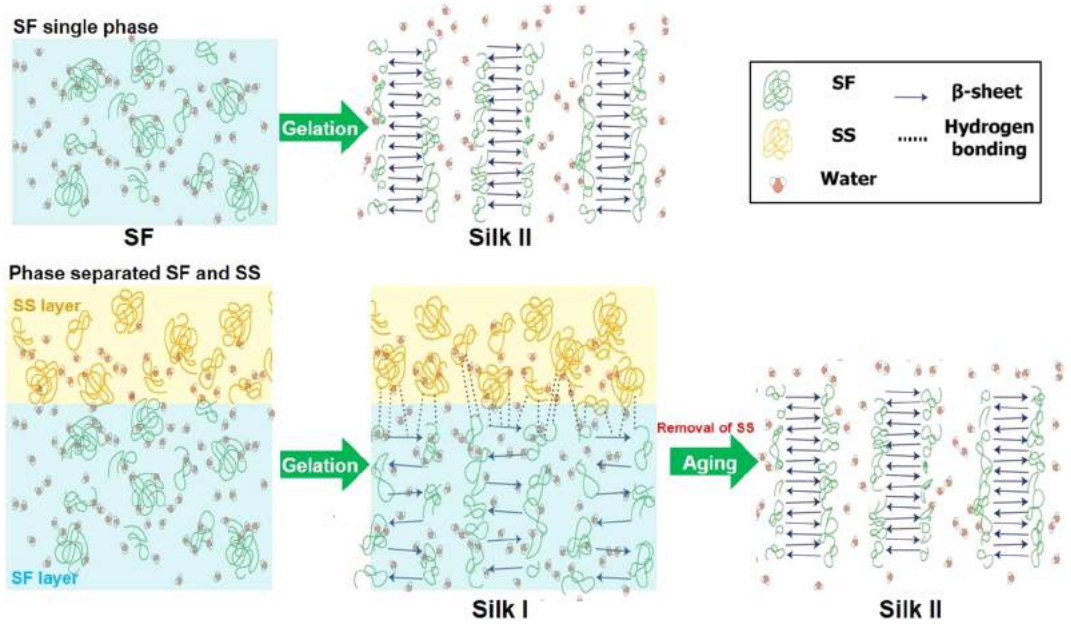

Figure 8. Schematic of the effect of phase-separated silk sericin (SS) on the conformational transition of silk fibroin (SF).

structures were insoluble in PBS. When subjected to enzymatic degradation, fibroin hydrogels prepared with an upper phase-separation of distilled water and 0.25% sericin solution had greater stability against enzymatic degradation, which indicates Silk II structure formation. On the other hand, fibroin hydrogels prepared with phase-separated 0.50% and 1.00% sericin could be enzymatically degraded, indicating the existence of Silk I structures and backing up our XRD data.

Combined these results clearly show that the presence of a sericin layer induces the Silk I structure in fibroin hydrogels. This interaction has to occur at the interface between sericin and fibroin. Unfortunately, due to limited analysis techniques, it is difficult to identify precisely the nature of the sericin and fibroin interaction. However, we can now begin to speculate based our data and evidence from other reports. Lee[14] has reported retardation of fibroin crystallization in the presence of sericin in films. Ki et al.[12] reported the effect of sericin on the secondary structure of fibroin during wet spinning, and Hang et al.[13] suggested some interaction between sericin and fibroin during coaxial electrospinning. Their findings indicate that sericin can affect the structural transition of fibroin at an interface. Based on current and former results, the following mechanism is suggested for the development of Silk I structures from fibroin in the presence of sericin. It has been reported that the gelation of fibroin results from the conformational transition from random coil to β-sheet structures.[38] During this process, the hydrophobic part of fibroin, which consists of repeated sequences, will start to agglomerate in order to avoid an unfavorable aqueous environment. The process will continue until they find the most thermodynamically stable state, typically adopting a β-sheet conformation (Silk II), which also acts as a physical cross-linker in the fibroin hydrogel. However, we believe the interaction between fibroin and sericin at the interface may affect the self-assembly of fibroin. This type of intervention by structure can be observed in other self-assembling peptides. The Stupp group has studied the self-assembly of peptide-amphiphiles and found that the β-sheet-stabilized self-assembly could only be found when the sequence was maintained.[39] Therefore, even a slight disruption in the hydrogen-bonding pattern of fibroin may prevent its β-sheet formation, which we propose to be caused by sericin (Figure 8). Here, this was seen by a promotion of Silk I structures in fibroin rather than the usually more stable Silk II. This was then confirmed as upon removal of the sericin layer, the Silk I structure of fibroin converted into Silk II.

From a biological perspective, the influence of sericin on fibroin may have profound effects. Like the gelation observed in this study, natural spinning surrounds a conformational transition of fibroin from a Silk I structure to a Silk II.[40] Therefore, prior to spinning, the Silk I structure is the typical structure of fibroin in the silk gland. Yet, this has been difficult to characterize in the past due to its inherent instability and tendency to convert into Silk II. Our current results suggest that sericin may be responsible for inducing and maintaining the Silk I structure in the animal prior to spinning, despite being phase-separated. Until now, its role was underestimated as simply being a lubricant. However, the current results indicate that sericin may have a further role in preventing premature fibroin crystallization in the gland.

4. CONCLUSIONS

Silk sericin may have more important roles than has been previously been recognized. In this study, a phase-separated fibroin and sericin solution layer was constructed to mimic the conditions inside in the middle of the silk gland. It was found that phase-separated sericin slowed the gelation of fibroin, and this became more significant as the sericin concentration increased. From ThT fluorescence intensity kinetics and ATR-FTIR measurements, this delay in gelation correlated with slow β-sheet structure development in the fibroin layer with XRD indicating a Silk I structure was promoted instead. Subsequent mechanical property tests and degradation studies highlighted that not only structure, but other physical properties were influenced by sericin. These results suggest that sericin, even though it was phase-separated, could prevent premature crystallization of fibroin and induce a Silk I hydrogel structure. Interpreting these findings in a wider context of the natural system, we propose that in the silk gland the sericin layer that

DOI: 10.1021/acs.biomac.7b00549
Biomacromolecules 2017, 18, 2343−2349

surrounds the fibroin acts to stabilize the metastable fibroin before spinning. These findings could therefore have impact in the future storage and processing of fibroin and any biomimetic technological applications where careful control over the conversion and solidification of fibroin is required.

■ ASSOCIATED CONTENT

Supporting Information

The Supporting Information is available free of charge on the ACS Publications website at DOI: 10.1021/acs.biomac.7b00549.

Effect of silk sericin (SS) concentration on the concentration changes of each bottom and upper layer during the gelation of silk fibroin (SF; Figure S1). Effect of silk sericin (SS) (0.50%, w/v) on the increase in gelation time at different silk fibroin (SF) concentrations (Figure S2). Effect of phase-separated silk sericin (SS) on the secondary structure (a) and XRD crystal properties of silk fibroin (SF); (b) during the initial 1 h incubation period (Figure S3). Effect of phase-separated silk sericin (SS) on the secondary structure (a) and XRD crystal properties of silk fibroin (SF); (b) during further 48 h aging without upper sericin phase (Figure S4). Water dissolution and enzymatic degradation properties of silk fibroin (SF) gel phase-separated with different concentration of silk sericin (SS) and further incubation without upper layer for 48 h (Figure S5; PDF).

■ AUTHOR INFORMATION

Corresponding Author

*E-mail: prolee@snu.ac.kr.

ORCID

Ki Hoon Lee: 0000-0002-7364-3221

Present Address

‡Department of Materials Science and Engineering, The University of Sheffield, Sheffield, S1 3JD, U.K.

Author Contributions

The manuscript was written through contributions of all authors. All authors have given approval to the final version of the manuscript.

Notes

The authors declare no competing financial interest.

■ ACKNOWLEDGMENTS

This work was supported by the Basic Science Research Program through the National Research Foundation of Korea (NRF), funded by the Ministry of Education (NRF-2010-0025378 and NRF-2013R1A1A2059239) and the EPSRC, Project Reference EP/K005693/1.

■ REFERENCES

(1) Koeppel, A.; Holland, C. *ACS Biomater. Sci. Eng.* **2017**, *3* (3), 226−237.
(2) Werner, V.; Meinel, L. *Eur. J. Pharm. Biopharm.* **2015**, *97*, 392−399.
(3) Melke, J.; Midha, S.; Ghosh, S.; Ito, K.; Hofmann, S. *Acta Biomater.* **2016**, *31*, 1−16.
(4) Vollrath, F.; Porter, D.; Holland, C. *MRS Bull.* **2013**, *38* (1), 73−80.
(5) Ki, C. S.; Park, Y. H.; Jin, H.-J. *Macromol. Res.* **2009**, *17* (12), 935−942.
(6) Aramwit, P.; Siritientong, T.; Srichana, T. *Waste Manage. Res.* **2012**, *30* (3), 217−224.
(7) Lamboni, L.; Gauthier, M.; Yang, G.; Wang, Q. *Biotechnol. Adv.* **2015**, *33* (8), 1855−1867.
(8) Laity, P. R.; Gilks, S. E.; Holland, C. *Polymer* **2015**, *67*, 28−39.
(9) Holland, C.; Terry, A. E.; Porter, D.; Vollrath, F. *Polymer* **2007**, *48* (12), 3388−3392.
(10) Jin, H.-J.; Kaplan, D. L. *Nature* **2003**, *424* (6952), 1057−1061.
(11) Zhong, J.; Liu, X.; Wei, D.; Yan, J.; Wang, P.; Sun, G.; He, D. *Int. J. Biol. Macromol.* **2015**, *76*, 195−202.
(12) Ki, C. S.; Park, Y. H. *Fibers Polym.* **2013**, *14* (9), 1460−1467.
(13) Hang, Y.; Zhang, Y.; Jin, Y.; Shao, H.; Hu, X. *Int. J. Biol. Macromol.* **2012**, *51* (5), 980−986.
(14) Lee, K. H. *Macromol. Rapid Commun.* **2004**, *25* (20), 1792−1796.
(15) Takasu, Y.; Yamada, H.; Tsubouchi, K. *Biosci., Biotechnol., Biochem.* **2002**, *66* (12), 2715−2718.
(16) Matsumoto, A.; Chen, J.; Collette, A. L.; Kim, U.-J.; Altman, G. H.; Cebe, P.; Kaplan, D. L. *J. Phys. Chem. B* **2006**, *110* (43), 21630−21638.
(17) Hu, X.; Kaplan, D.; Cebe, P. *Macromolecules* **2006**, *39* (18), 6161−6170.
(18) Yun, H.; Kim, M. K.; Kwak, H. W.; Lee, J. Y.; Kim, M. H.; Lee, K. H. *Int. J. Biol. Macromol.* **2016**, *82*, 945−951.
(19) Zhang, H.; Deng, L.; Yang, M.; Min, S.; Yang, L.; Zhu, L. *Int. J. Mol. Sci.* **2011**, *12* (5), 3170−3181.
(20) Kunz, R. I.; Brancalhao, R. M. C.; Ribeiro, L. F. C.; Natali, M. R. M. *BioMed Res. Int.* **2016**, *2016*, e8175701.
(21) Dai, P.; Iwashita, Y.; Kawasaki, H. *Nippon Sanshigaku Zasshi* **1994**, *63* (2), 149−156.
(22) Oh, H.; Kim, M. K.; Yi, J.; Lee, K. H. *J. Korean Fiber Soc.* **2009**, *46* (5), 289−294.
(23) Tansil, N. C.; Koh, L. D.; Han, M.-Y. *Adv. Mater.* **2012**, *24* (11), 1388−1397.
(24) Kwak, H. W.; Lee, K. H. *Int. J. Indust. Entomol.* **2015**, *30* (1), 1−5.
(25) Hou, Y.; Li, P.; Zhou, H.; Zhu, X.; Chen, H.; Lee, J.; Koh, K.; Shen, Z.; Chen, H. *J. Nanosci. Nanotechnol.* **2015**, *15* (2), 1110−1116.
(26) Jiang, T.; Zhou, G.-R.; Zhang, Y.-H.; Sun, P.-C.; Du, Q.-M.; Zhou, P. *RSC Adv.* **2012**, *2* (24), 9106−9113.
(27) Yao, T.; Jiang, T.; Pan, D.; Xu, Z.-X.; Zhou, P. *RSC Adv.* **2014**, *4* (76), 40273−40280.
(28) Wang, J.; Zhang, S.; Xing, T.; Kundu, B.; Li, M.; Kundu, S. C.; Lu, S. *Int. J. Biol. Macromol.* **2015**, *79*, 316−325.
(29) Groenning, M. *J. Chem. Biol.* **2010**, *3* (1), 1−18.
(30) Floren, M. L.; Spilimbergo, S.; Motta, A.; Migliaresi, C. *Biomacromolecules* **2012**, *13* (7), 2060−2072.
(31) Lu, Q.; Hu, X.; Wang, X.; Kluge, J. A.; Lu, S.; Cebe, P.; Kaplan, D. L. *Acta Biomater.* **2010**, *6* (4), 1380−1387.
(32) Nagarkar, S.; Nicolai, T.; Chassenieux, C.; Lele, A. *Phys. Chem. Chem. Phys.* **2010**, *12* (15), 3834.
(33) Kim, H. H.; Song, D. W.; Kim, M. J.; Ryu, S. J.; Um, I. C.; Ki, C. S.; Park, Y. H. *Polymer* **2016**, *90*, 26−33.
(34) Numata, K.; Katashima, T.; Sakai, T. *Biomacromolecules* **2011**, *12* (6), 2137−2144.
(35) Wray, L. S.; Hu, X.; Gallego, J.; Georgakoudi, I.; Omenetto, F. G.; Schmidt, D.; Kaplan, D. L. *J. Biomed. Mater. Res., Part B* **2011**, *99B* (1), 89−101.
(36) Gil, E. S.; Park, S.-H.; Hu, X.; Cebe, P.; Kaplan, D. L. *Macromol. Biosci.* **2014**, *14* (2), 257−269.
(37) Lu, Q.; Zhang, B.; Li, M.; Zuo, B.; Kaplan, D. L.; Huang, Y.; Zhu, H. *Biomacromolecules* **2011**, *12* (4), 1080−1086.
(38) Ayub, Z. H.; Arai, M.; Hirabayashi, K. *Biosci., Biotechnol., Biochem.* **1993**, *57* (11), 1910−1912.
(39) Korevaar, P. A.; Newcomb, C. J.; Meijer, E. W.; Stupp, S. I. *J. Am. Chem. Soc.* **2014**, *136* (24), 8540−8543.
(40) Andersson, M.; Johansson, J.; Rising, A. *Int. J. Mol. Sci.* **2016**, *17* (8), 1290.

DOI: 10.1021/acs.biomac.7b00549
Biomacromolecules 2017, 18, 2343−2349